Environ Sci Pollut Res (2016) 23:17474–17483
DOI 10.1007/s11356-016-6852-5

RESEARCH ARTICLE

Global Mercury Observatory System (GMOS): measurements of atmospheric mercury in Celestun, Yucatan, Mexico during 2012

Antonio Velasco[1] · **Flor Arcega-Cabrera**[2] · **Ismael Oceguera-Vargas**[2] · **Martha Ramírez**[1] · **Abraham Ortinez**[1] · **Gunther Umlauf**[3] · **Fabrizio Sena**[3]

Received: 14 May 2015 / Accepted: 9 May 2016 / Published online: 27 May 2016

Abstract Within the Global Mercury Observation System (GMOS) project, long-term continuous measurements of total gaseous mercury (TGM) were carried out by a monitoring station located at Celestun, Yucatan, Mexico, a coastal site along the Gulf of Mexico. The measurements covered the period from January 28th to October 17th, 2012. TGM data, at the Celestun site, were obtained using a high-resolution mercury vapor analyzer. TGM data show values from 0.50 to 2.82 ng/m^3 with an annual average concentration of 1.047 ± 0.271 ng/m^3. Multivariate analyses of TGM and meteorological variables suggest that TGM is correlated with the vertical air mass distribution in the atmosphere, which is influenced by diurnal variations in temperature and relative humidity. Diurnal variation is characterized by higher nighttime mercury concentrations, which might be influenced by convection currents between sea and land. The back trajectory analysis confirmed that local sources do not significantly influence TGM variations. This study shows that TGM monitoring at the Celestun site fulfills GMOS goals for a background site.

Responsible editor: Philippe Garrigues

✉ Flor Arcega-Cabrera
farcega@unam.mx

[1] Instituto Nacional de Ecología y Cambio Climático (INECC), Periférico 5000 Col. Insurgentes Cuicuilco, Delegación Coyoacán, CP 04530 México, D.F., Mexico

[2] Unidad de Química Sisal, Facultad de Química, Universidad Nacional Autónoma de México, Puerto de Abrigo s/n, Sisal, Yucatán 97355, Mexico

[3] European Commission-Joint Research Centre, Institute for Environment and Sustainability (IES), Via Enrico Fermi, 2749, 21027 Ispra, Italy

Keywords Total gaseous mercury · Global Mercury Observation System · Time series · Diurnal variations · Atmospheric transport · Multivariate analysis · Background site

Introduction

Mercury (Hg) in its elemental form is considered a global pollutant due to its environmental persistence, ecotoxicity, and ability to bio-accumulate in the human food chain (Mason et al. 1995). Hg is also classified as a priority pollutant under national, regional, and international conventions such as United Nations Environment Programme (UNEP)-Minamata convention, United Nations Economic Commission for Europe (UNECE) convention, and OSPAR (Convention for the Protection of the Marine Environment of the North-East Atlantic) convention or the European Water Framework Directive. All of which aim to reduce the adverse effects of mercury on human health and the environment (Pirrone and Mason 2009; Sprovieri et al. 2013).

Mercury is released into the environment by both natural and anthropogenic sources around the world. Volcanoes, soil and water surfaces, Earth crust weathering processes, and forest fires are among the most important natural sources of mercury. Anthropogenic sources include mainly burning of fossil fuels, manufacturing processes involving ferrous and non-ferrous metals, production of chemicals, processing of ores, treatment of waste, and cement production (Lu and Schroeder 2004; Pirrone and Mason 2009; UNEP 2013). The atmosphere is a major vector in the transformation and transport of mercury from emission sources to receptors. Mercury in the atmosphere exists in three forms: gaseous elemental mercury (GEM), reactive gaseous species (RGM), and particulate mercury (Hg_P). The reactive and particulate forms have a short

permanence in the atmosphere. This is the case because they are marked by fast wet and dry deposition, and their transport occurs over a limited distance from a source. GEM has a longer lifetime (estimated atmospheric permanence between 0.5 and 2 years (Lindqvist and Rodhe 1985), resulting in more dispersion time and global transport (Schroeder and Munthe 1998; Poissant 2000; Weiss-Penzias et al. 2003). The persistence and predominance (generally, over 95 %) of elemental mercury in air is attributed to its comparatively high-vapor pressure, low solubility in water, and high chemical stability (Kim et al. 1987; Carpi and Lindberg 1998). Atmospheric transport and longer lifetime are the main factors promoting the presence of Hg in remote regions (such as the Arctic and Antarctica) (Brosset 1987; Iverfeldt 1991; Petersen et al. 1995). In general terms, as well as in this paper, total concentration of elemental mercury in air is reported as total gaseous mercury (TGM), which is the sum of GEM and RGM.

Several regional, national, and international programs are collecting high-quality atmospheric Hg data (e.g., European Monitoring and Evaluation Program (EMEP), Canadian Atmospheric Mercury Measurement Network (CAMNet), Artic Monitoring and Assessment Program (AMAP), and National Atmospheric Deposition Program-Mercury Deposition Network (NADP-MDN)). However, in reality, it is extremely difficult to analyze long-term global trends in mercury across the northern and southern hemispheres due to the lack of a coordinated monitoring network (Sprovieri et al. 2010). For this reason, the Global Mercury Observation System (GMOS) is taking the lead in developing the first global-scale ground-based network of Hg monitoring sites. The network, financed by the European Commission's 7th Framework Programme for Research, provides continuous information on mercury concentrations, temporal trends, and fluxes among atmospheric, marine, freshwater, and terrestrial ecosystems. This information has a positive and immediate impact on policy makers concerned with implementing strategies to reduce the adverse effects of mercury on human health and the environment (GMOS 2013; Sprovieri et al. 2013).

The inclusion of developing and transitional countries, such as Mexico, in GMOS is of relevance since there is a lack of information on atmospheric mercury from sites within these countries. Until recently, Hg measurement databases were limited in many regions, including Mexico. Importantly, they are necessary in order to construct a representative Hg monitoring network where geographical variation and long-term trends can be identified.

The present research reports on long-term continuous monitoring of TGM at Celestun, Yucatan, to determine whether or not this site can function as a background monitoring location or a reference location for comparison with measurements taken on or near an emission site (Fritz et al. 2015) and following GMOS's standards and goals. Specifically, these standards and goals include (among others): (1) recording ambient concentrations and deposition fluxes of mercury species and (2) understanding the processes that contribute to Hg variability on a diurnal, weekly, seasonal, and annual basis.

Methods

A Total Gaseous Mercury monitoring station was established in 2011 as part of the GMOS project. Air data from January 28 to October 17, 2012 were obtained and analyzed to identify daily and monthly variations in Hg. Multivariate analyses were performed to explore the processes affecting or directing variations (Arcega-Cabrera et al. 2009, 2014, 2015). Back trajectory analysis was performed in order to evaluate contaminant transport. Finally, data were compared with worldwide data from other GMOS sites in order to establish Celestun as a background site.

Site description

The station was located at the "*John E. Walker*" *Center for Research and Training on Natural Resources* owned by Ducks Unlimited de Mexico, A.C. (DUMAC) in Celestun, Yucatan (Fig. 1). The DUMAC Center is located about 1.9 km away from the Gulf of Mexico coast and 1.4 km from the town of Celestun. The site is situated inside the Celestun Biosphere Reserve, which is an extensive wetland (147,500 acres) that hosts flamingos, herons, and other bird species during the winter. The reserve contains a mixture of tropical savanna, low tropical subdeciduous forest, and *tular* vegetation. The predominant economic activities in Celestun are tourism, fishing, and salt extraction. The most probable mercury emission sources that might contribute to the presence of mercury in the atmosphere are located more than 70 km away from the site, as shown in Table 1 (Marquez-Estrada 2011). However, in the state of Yucatan, burning of domestic waste, in uncontrolled dumps and household garbage in backyards, is widely practiced throughout the year. Burning of secondary vegetation in agricultural areas takes place mainly from March to May (SEDUMA-Yucatán 2009). Both processes release Hg into the atmosphere.

The DUMAC Center consists of a two-floor concrete structure equipped with metal fences. The terrain is flat, with calcareous soil and there are trees and shrubs.

An Automatic Weather Station (AWS) has been installed on the roof of the main building since 2000. This station is operated by the National Meteorological Service of Mexico, which transmits data via satellite to their headquarters in Mexico City.

The mercury analyzer was installed inside a plastic outdoor storage shed, on the roof of the main building close to the meteorological station. An air conditioner was installed in

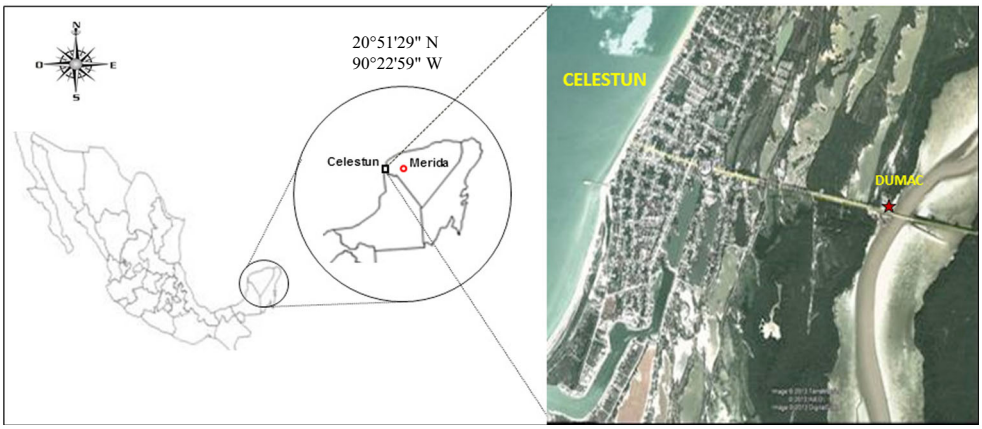

Fig. 1 Location of monitoring site at Celestun, Yucatan, Mexico

order to maintain the temperature inside the shed between 28 and 30 °C. The TGM sampling head was installed 10 m above the roof of the metallic structure of the meteorological station supporting it.

Measurement of TGM and meteorological parameters

A Tekran model 2537B automatic mercury-vapor analyzer took measurements of TGM in ambient air. The instrument was calibrated every 72 h with an internal automatic permeation source, which provides a known amount of mercury into a stream of mercury free air. Zero air was used for the instrument blank. The analyzer operated with a sampling time of 5-min and 1 L/min sample flow, providing a TGM detection range from 0.1 to 2000 ng/m^3. Weekly routine maintenance was conducted to ensure proper operation of the equipment throughout the study period.

Mercury measurement and data validation were performed according to GMOS's quality assurance and quality control system (QA/QC), which are based on standard operational procedures and guidelines (GMOS 2013).

The meteorological parameters of temperature (T), solar radiation (SR), barometric pressure (P), relative humidity (RH), wind direction (WD), and wind speed (WS) were recorded and transmitted automatically by Forest Technology Systems (FTS) brand weather station. The sensors used by the FTS station meet NFDRS/CFDRS standards, reporting averages of all of the variables every 10 min. They consist of a SDI RM Young Wind Monitor for wind speed and direction, a SDI-1S for barometric pressure, a THS-3 for temperature and relative humidity, a Pyranometer for solar radiation, and a RG-T rain gauge for precipitation.

Statistical analysis

The diurnal cycle in Hg concentration was calculated as the average value for each hour of the time series.

Multivariate analyses on log-transformed data (to avoid bias by magnitude or variable type) were done to explore the processes affecting or directing variation in TGM. STATSoft's STATISTICA program was used for statistical analysis following Arcega-Cabrera et al. (2009, 2014, 2015); also see García et al. 2006, for example. Cluster analysis (CA), with Ward's method and Pearson's correlation, principal components analysis (PCA), and factor analysis were utilized.

Back trajectories

Back trajectories of air masses were calculated using HYSPLIT-4 model from National Oceanic and Atmospheric Administration (NOAA) (Draxler 1999). The Global Data Assimilation (GDAS) set was used as meteorological input. Trajectories from highest and lowest mercury concentrations events were modeled at heights of 20, 500, and 1500 m amsl.

Table 1 Mercury emission stationary sources in Merida city

Emission sources	Sites	Distance from monitoring site (km)
Electric power plants	4	72,73, 84 and 221
Lime Kilns	2	77 and 88
Incinerator of biological hazardous wastes	1	82
Metallurgical plants	2	74 and 83
Cement plant	1	76
Crematoria	1	70

Air mass flows at the monitoring mercury station were observed at 20 m amsl. HYPSLIT-4 then modeled TGM at 500 m amsl, which corresponds with transport from local sources, and at 1500 m amsl, which marks the transition between local and regional transport. It is important to mention that the station is located on an enormous coastal plain; thus, the absence of topographic features allowed for terrain effects to be dismissed.

Results and discussion

Overall TGM concentration

TGM concentration values from January 28 to October 17, 2012 are plotted in Fig. 2 and range from 0.50 to 2.82 ng/m^3. Table 2 shows the overall mean TGM concentration of 1.05 ± 0.27 ng/m^3 calculated from 44,537 individual data points, with the maximum value of 2.822 ng/m^3 observed in March.

Mean TGM concentrations reported in this research are slightly lower than the values obtained during short-term sampling campaigns at others Mexican sites. Puerto Angel, Oaxaca located on the Pacific Coast, is considered a remote site, while Huejutla, Hidalgo, located in the central Gulf coast region, is considered a remote rural site. These sites had average values of 1.46 and 1.32 ng/m^3 respectively (De la Rosa et al. 2004).

Table 3 shows TGM values registered at some remotes sites around the world. Comparing the atmospheric mercury content with other regions in the world, TGM mean annual concentration in Celestun is closer to the Southern Hemisphere background concentration, rather than the Northern Hemisphere range reported by Lindberg et al (2007). The Celestun values are similar to the average value reported for Cape Point, Cape Peninsula, South Africa, for the 2007–2008 period. According to Brunke et al. (2010), Cape Point is representative of clean maritime air coming from the Southern Ocean.

Meteorological data trends

Table 4 shows the descriptive statistics for the annual meteorological data registered during 2012. The median annual temperature, relatively humidity, and atmospheric pressure values are 26.3 °C, 71.0 %, and 1013.2 hPa, respectively. The 25th and 75th percentiles in the meteorological data distribution during 2012 are: 24.4 and 28.8 °C for temperature, 60 and 80 % for relative humidity, and 1011.2 and 1015.2 hPa for barometric pressure.

Figure 3 shows monthly prevailing wind direction and wind speed at the Celestun site. Monthly wind pattern indicates that, from January to May, winds are predominantly from North–Northeast (NNE) and Southeast (SE). From June to September, prevailing winds are from the East (E), and from October to November, the prevalent directions are from the East and Northeast (NE). Wind speed was typically around 11 m/s at the Celestun site. Based on data recorded between 2000 and 2007 from nine meteorological stations, located on the Yucatan Peninsula, Soler-Bientz et al. (2010) indicated that prevailing winds come from directional sectors between North–Northeast (NNE) (i.e., from the eastern Gulf of Mexico) and East–Southeast (ESE) (i.e., from the western Caribbean). This study mentioned that atmospheric stability over these water bodies causes the winds to arrive on the Yucatan Peninsula. They also found that the Celestun site exhibited high winds speed (around 9 m/s) due to the combined effect of prevailing winds coming off the peninsula and

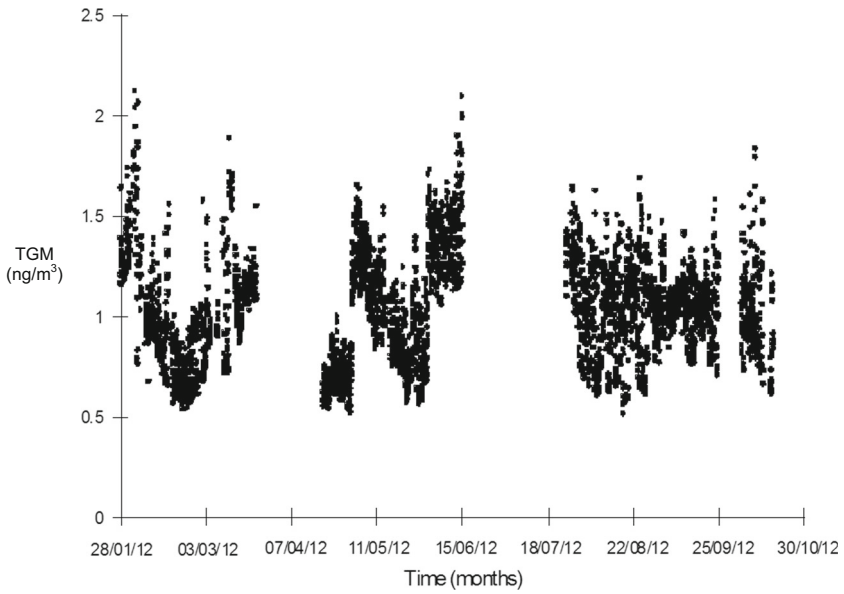

Fig. 2 Time series of TGM concentration during 2012

Table 2 TGM values in Celestun site

Month	Data number (*n*)	TGM (ng/m^3)				
		Min	Max	Mean	Median	Standard deviation
February	5790	0.501	2.628	0.972	0.903	0.315
March	4690	0.500	2.822	1.083	1.047	0.270
April	2782	0.500	1.330	0.752	0.748	0.177
May	7885	0.500	1.878	1.028	1.034	0.255
June	4096	0.715	2.235	1.388	1.385	0.200
July	1351	0.675	1.783	1.232	1.256	0.213
August	8760	0.512	1.791	1.026	1.047	0.230
September	6707	0.649	1.720	1.054	1.057	0.145
October	2476	0.619	2.000	1.035	1.005	0.212
Annual	44,537	0.500	2.822	1.052	1.047	0.271

winds from the Gulf of Mexico and the Caribbean. The prevailing maritime air, which comes from the Caribbean, coupled with the high wind speed in this region, may explain the low TGM concentrations detected at the Celestun site.

Diurnal and temporal variation in TGM concentrations

Diurnal fluctuation in TGM was observed mainly during May, August, and September. Diurnal TGM patterns were characterized by the highest TGM concentrations during the night as opposed to during the day (see Fig. 6). The highest mercury levels were registered between 0300 and 0600 local time, while the lowest TGM values were observed from 1400 to 1800 local time. In contrast, temperature followed the opposite pattern, lowest during the night and highest during the day. Furthermore, the inverse correlation between temperature and TGM content revealed by the multivariate analysis (see below) is also evident in Fig. 6.

Table 3 TGM concentration registered in some remotes sites around the world

Remote sites	TGM concentration (ng/m^3)	Reference
North hemisphere	1.5 to 1.7	Lindberg et al. 2007
Arctic Ocean in the North Atlantic	1.53 ± 0.12	Aspmo et al. 2006
South hemisphere	1.1 to 1.3	Lindberg et al. 2007
Antarctic	1.08 ± 0.29	Temme et al. 2003
Mt. Waliguan Observatory China	1.7 ± 1.1 (Summer time)	Wang et al. 2007
Cape Point, Cape Peninsula, South Africa	0.944 ± 0.160	Brunke et al. 2010
Celestun, Yucatan, Mexico	1.047 ± 0.271	This study

The differential between high and low peaks in TGM is within a range of 0.4 ng/m^3. Kellerhals et al. (2003) indicated that diurnal fluctuations in TGM are the result of complex physical and chemical processes involving surface deposition, volatilization from surrounding surfaces, and transport. Several authors have reported TGM diurnal variations. Zhu et al. (2012) and Fu et al. (2008) registered the highest TGM concentration during the day, while Lee et al. (1998) and Schmolke et al. (1999) registered it during the night. Schmolke et al. (1999) mentioned that nighttime peaks in TGM concentrations can be attributed to surface mercury emissions that accumulate with nocturnal inversion.

Due to the particular geographical position of the Celestun site (i.e., close to the coast), TGM diurnal fluctuations are likely the result of convective currents produced as a consequence of the temperature gradient between the land and sea surface. This gradient promotes a diurnal change in local wind circulation. During the day, warn air rises from the land, creating convection, which generates a breeze from sea to land (onshore flow), whereas at night warm air rises from the sea, which inverts the convection and generates a breeze from land to

Table 4 Meteorological values registered during 2012

	T (°C)	RH (%)	BP (hPa)
Mean	26.6	69.4	1013.2
Median	26.3	71.0	1013.2
Std dev	3.1	13.0	2.91
Min	16.8	24.0	1004.6
Max	35.8	91.0	1024.7
Q25	24.4	60.0	1011.2
Q75	28.8	80.0	1015.2
P10	22.8	52.0	1009.4
P90	30.8	85.0	1016.8

$N = 5462$

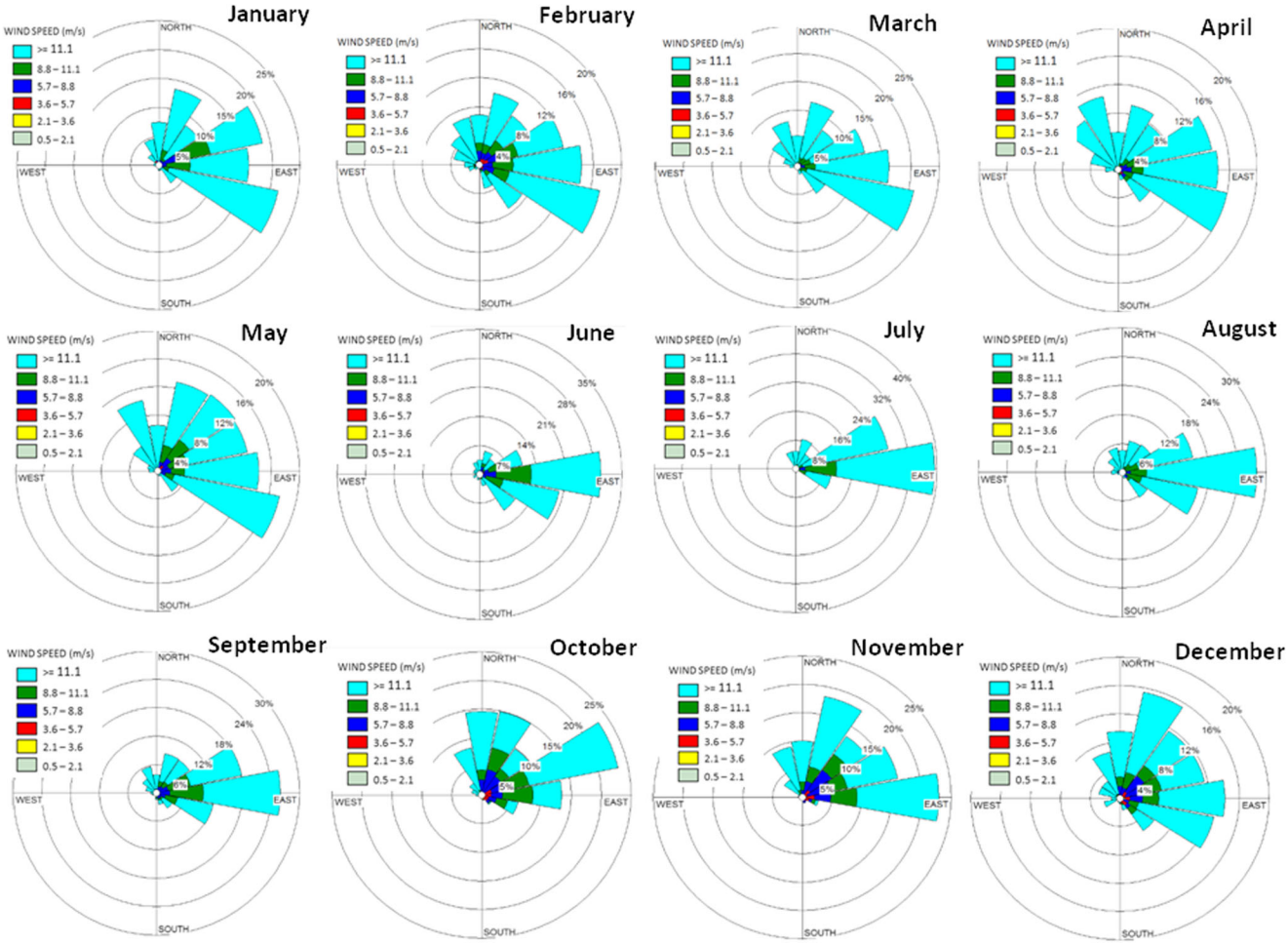

Fig. 3 Prevalent wind directions in Celestun site, 2012

sea (offshore flow) (Kennett et al. 2001). This phenomenon could explain higher nighttime TGM concentrations.

Average monthly TGM concentrations show no significant differences ($p < 0.05$), indicating non-significant temporal

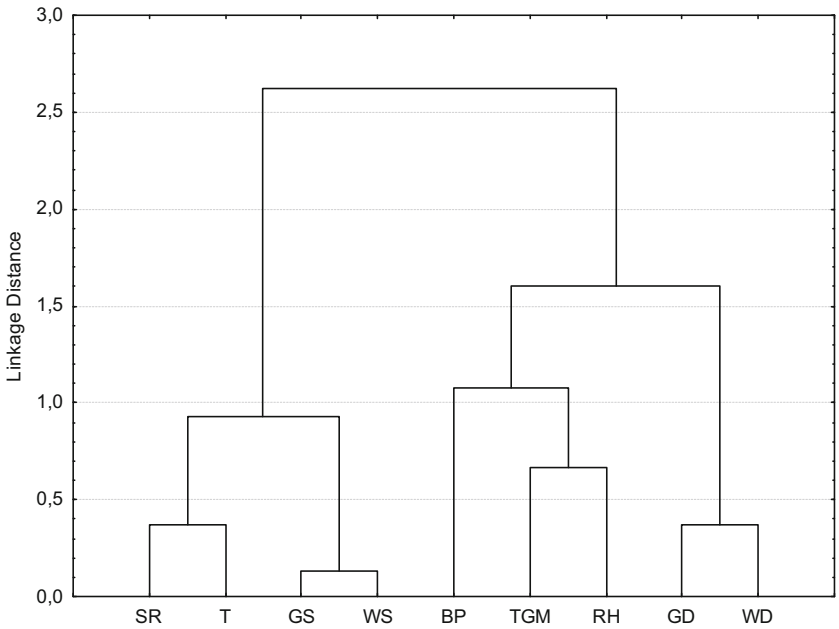

Fig. 4 Cluster analysis for 10 variables. Ward's method with Pearson's correlation was used

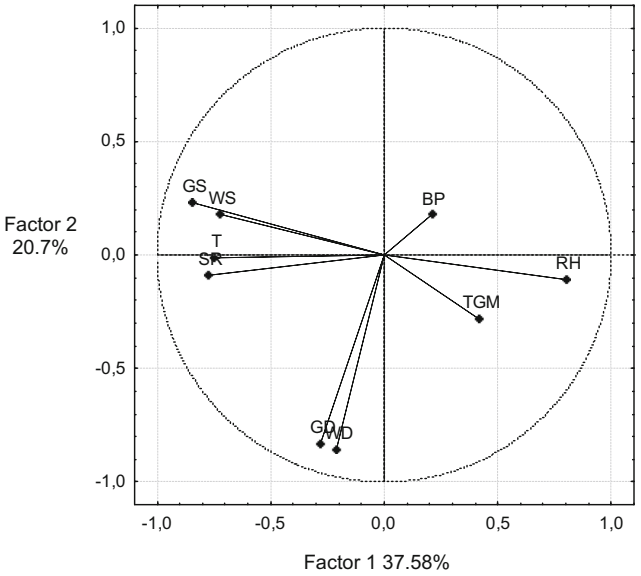

Fig. 5 Projection of variables on 2D plane. Explained variability = 58.28 %

variation in TGM levels throughout the year at the Celestun site. Some studies (Kock et al. 2005; Stamenkovic et al. 2007; Wan et al. 2009) mentioned that seasonal variability in TGM concentrations could depend on seasonal differences in fossil fuel combustion, atmospheric-oxidant concentrations, mixing layer depth, and meteorological conditions. Conversely, temporal variability in TGM levels from Celestun show only punctual variations, which could be the result of smaller scale processes.

Relations among meteorological variables and TGM

Multivariate exploratory analyses were performed in order to further explain the relation among meteorological variables and TGM. Precipitation was excluded from analysis since the data represented less than 15 % of the total data; therefore, its relation with average TGM is insignificant, showing no tendencies. Cluster analysis formed three groups (Fig. 4): the first one encloses solar radiation (SR), temperature (T), and wind and gust speed (WS and GS respectively); the second group associates TGM (Hg), relative humidity (RH), and barometric pressure (BP); and, the third group, which is related with the second one, encloses wind and gust direction (WD and GD respectively). This analysis shows that the variables included in the second and third groups are the ones more likely directing variations in TGM. Principal component analysis (PCA) was also applied (Arcega-Cabrera et al 2009, 2014, 2015). Figure 5 shows the best mathematical approximation for the relation among the variables in each component. This projection explains more than 57 % of the observed variance. Component 1 (which explains 37.58 % of the variance) shows that variations in TGM are directly related with local atmospheric-column processes (RH, BP) and have a

Table 5 Factor analysis for Celestun site

	Factor 1	Factor 2	Factor 3
WD	0.00	*0.90*	0.03
GD	0.06	*0.89*	0.05
WS	*0.81*	0.07	0.03
GS	*0.89*	0.02	0.11
T	0.49	0.05	*0.74*
RH	*−0.72*	−0.05	−0.36
BP	0.12	−0.03	*−0.79*
SR	0.64	0.23	0.37
TGM	−0.56	0.09	0.14
Expl.Var	2.95	1.69	1.49
Prp.Totl	0.33	0.18	0.17

Significant values in italics >0.7, explained variability = 68 %

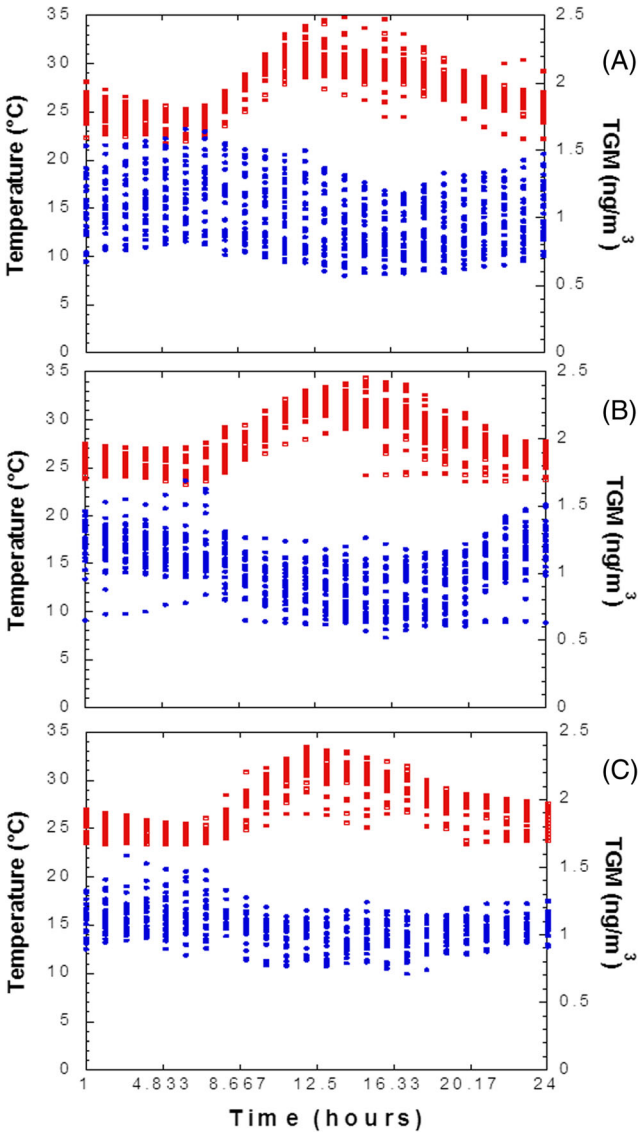

Fig. 6 Diurnal variation of TGM observed during May (**a**), August (**b**), and September (**c**) 2012 (temperature: *red squares*, TGM: *blue circles*)

close, but not totally clear, relation with wind and gust direction (WD, GD). On the other hand, Component 2 (which explains 20.7 % of the variance) indicates that TGM variations are inversely related with WS and GS, probably indicating dispersion processes. This component also showed an inverse relation with temperature and solar radiation, which probably explains the higher TGM values recorded during the night.

A factor analysis (FA) with a varimax-normalized rotation was performed in order to investigate the weight of each variable in TGM variations (Table 5). Three factors accounted for 68 % of the total variance. Factor 1 explained 33 % of the total observed variance. It shows that WS (loading = 0.81), GS (loading = 0.89), and SR (loading = 0.64) are inversely related with TGM (Hg, loading = −0.56), whereas RH (loading = −0.72) shows a direct relation with TGM. This factor might be indicating that TGM is influenced by (1) dispersion processes due to wind and gust speed (the higher the speed, the less the TGM), which is evidenced by their inverse relation with TGM, (and 2) diurnal variation, which is demonstrated by the inverse relation between TGM and SR, results in higher nighttime concentrations of TGM. In Factor 2, WD (loading = 0.9) and GD (loading = 0.89) showed no relation with TGM. This factor might suggest that TGM variations are not dependent on wind and gust direction. Factor 3 showed that BP (loading = −0.79) had an inverse relation with temperature (loading = 0.74), which might suggest that TGM variations are indirectly associated with changes in ambient conditions between day and night (canonical correlation analysis between Factor 1 and Factor 3 = 0.82).

Trajectory modeling

To further investigate Hg variations and wind direction, back trajectories were calculated for events when the highest and lowest mercury concentrations were observed during the year. Figures 6 and 7 show the hourly back trajectories of the low-concentration events detected on February 27th, April 19th, and August 17th. The back trajectory indicated that air masses arriving from the Caribbean passed over the city of Merida most of the time. Also, back trajectories for the lowest TGM concentrations (around 0.5 ng/m^3) indicate that winds arrived from clean marine air as well as passing over Merida. Additionally, Fig. 7a, c shows that low-concentration back trajectories, for the most part, had wide eastern and southeastern air mass flow contributions. However, Fig. 7b demonstrates that these air mass flow contributions also came from the north.

Figure 8 shows the plots of the high-level events (with TGM concentrations around 2.2 ng/m^3) on March 12th, August 24th, and October 10th. These back trajectories indicated that air masses were derived from local or regional terrestrial sources. Consistent with this, the plots of vertical wind distribution showed a high-pressure system in the Yucatan Peninsula, with air mass flow under 500 m amsl, at the time of these events. Lower traveling height of air masses can favor transport from nearby surface-emitting sources, which results in elevated TGM concentrations (Fu et al. 2012). Figure 8a, b also demonstrates that most high-concentration back trajectories were coming from the east, and Fig. 8c indicates arrival from the northeast. However, they are not broad in comparison with the low-concentration back trajectories. Thus,

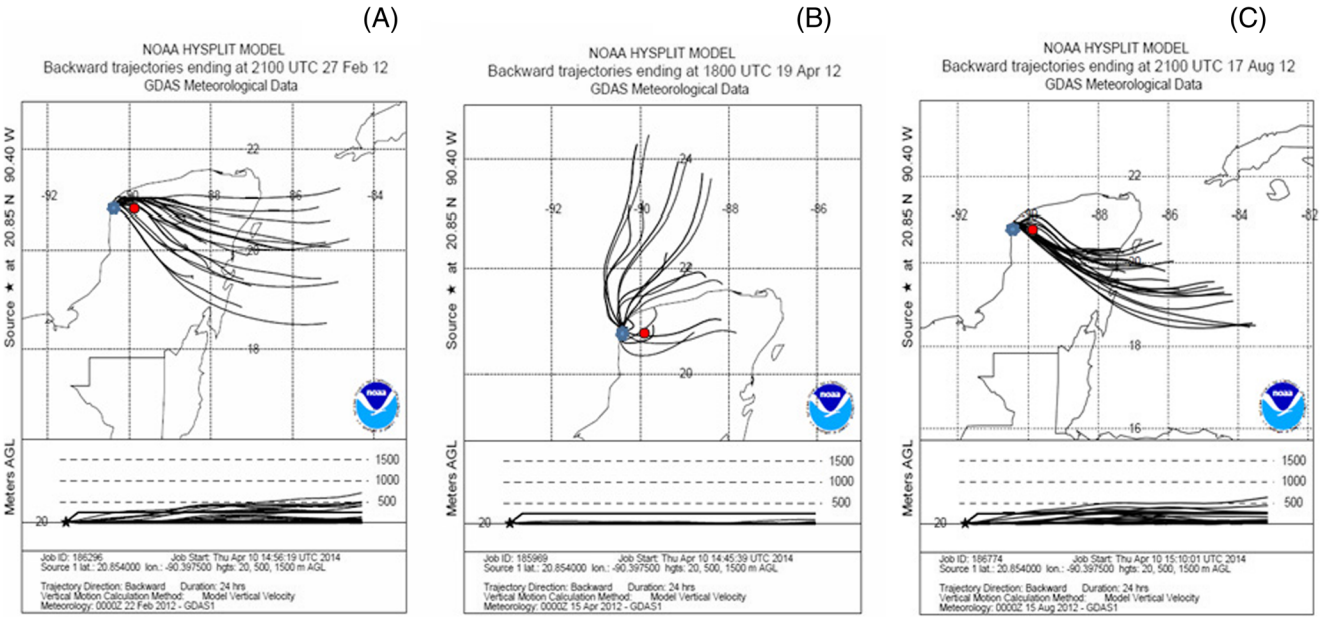

Fig. 7 Back trajectories associated with the lowest mercury levels during atmospheric mercury transport. Celestun (●), Merida (●). **a** UTC 27/02/12, **b** UTC 19/04/12, and **c** UTC 17/08/12

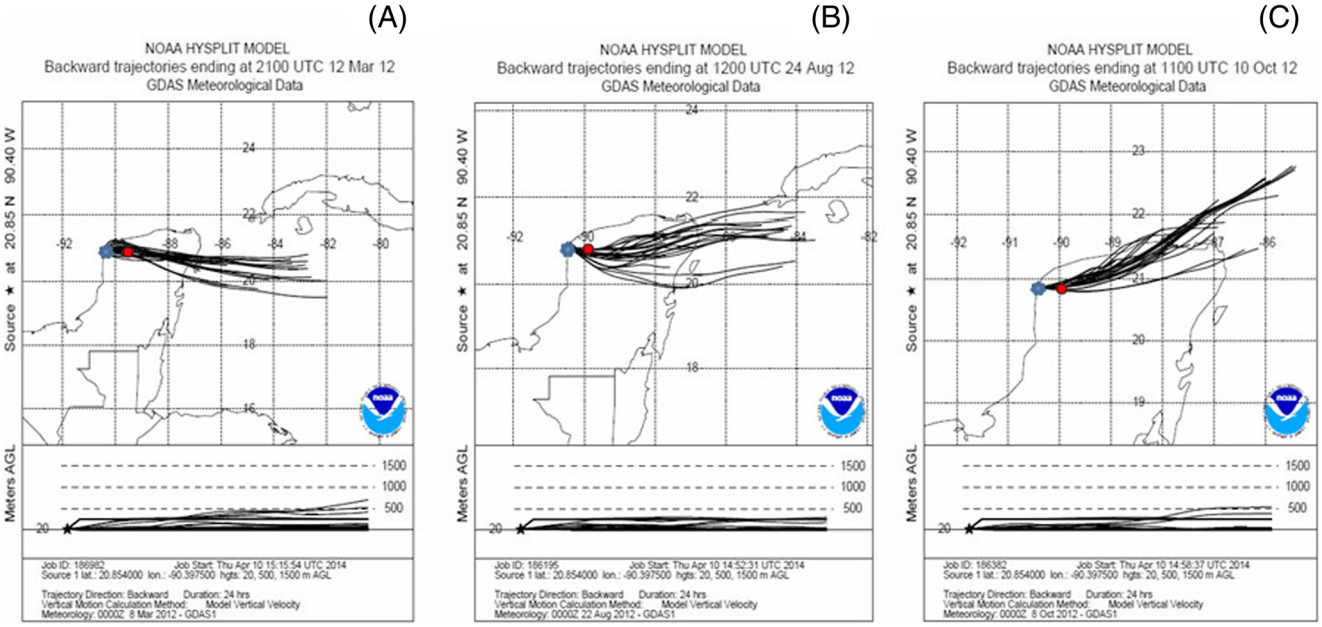

Fig. 8 Back trajectories associated with the highest mercury levels during atmospheric mercury transport. Celestun (●), Merida (●). **a** UTC 12/03/12, **b** UTC 24/08/12, and **c** UTC 10/10/12

together, Figs. 7 and 8 demonstrate that trajectories were not similar and showed different behaviors that might explain both high- and low-concentration scenarios. Also, the Yucatan Peninsula, during most of the year, is marked by high-pressure systems, which might contribution to air mass flow below 500 m amsl at the monitoring site.

These atmospheric conditions denote a non-significant influence of local sources located east of the station, while discarding regional contributions from Merida and maritime sources of the Gulf of Mexico and Caribbean. These results may indicate the influence of local anthropogenic activities involving agricultural burning, use of pesticides on citric crops, burning of backyard garbage, and domestic waste in informal dumps. Although these activities are common and widespread in many rural zones in Mexico, including municipalities in the State of Yucatan (SEDUMA-Yucatán 2009), they show a non-significant influence on the average mercury concentration registered at the Celestun site.

Conclusions

Mercury levels registered in this study suggest that Celestun is a good location for a global TGM background site. As well, variations in TGM recorded by this project will make an important contribution to a Hg measurement database for this region where no Hg data had been obtained previously. Long-term continuous monitoring of TGM in Celestun contributes to scholarly understand of the processes that promote Hg variability on a diurnal, monthly, and annual basis.

TGM ranged from 0.50 to 2.822 ng/m^3, with an annual average concentration of 1.047 ± 0.271 ng/m^3. Multivariate analyses show that TGM changes might be the result of two processes: (1) dispersion processes due to wind and gust speed and (2) a diurnal variation process, which causes nighttime TGM increases. Besides this, the back trajectories analysis confirmed that local anthropogenic sources located east of the station did not significantly influence TGM variation throughout the year.

In conclusion, TGM average yearly concentration showed non-significant variations. Therefore, data generated at this site can be use for comparative purposes, as well as regional and worldwide Hg modeling by the GMOS program.

Acknowledgments We would like to especially thank Nicola Pirrone, the director of the GMOS project, and his collaborator Francesca Sprovieri for their great support and the guidance they have provided for our work. We would also like to thank the DUMAC staff, from both Merida and Celestun, for their contributions in the management of the measuring station. This project received funding from the European Union's Seventh Programme for Research, Technological Development, and Demonstration under grant agreement No. 265113.

References

Arcega-Cabrera F, Armienta MA, Daesslé LW, Castillo-Blum SE, Talavera O, Dótor A (2009) Variations of Pb in a mine-impacted tropical river, Taxco, Mexico: use of geochemical, isotopic and statistical tools. Appl Geochem 24:162–171

Arcega-Cabrera F, Noreña-Barroso E, Oceguera-Vargas I (2014) Lead from hunting activities and its potential environmental threat to wildlife in a protected wetland in Yucatan, Mexico. Ecotoxicol Environ Saf 100:251–257

Arcega-Cabrera F, Garza-Pérez R, Noreña-Barroso E, Oceguera-Vargas I (2015) Impacts of geochemical and environmental factors on seasonal variation of heavy metals in a coastal lagoon Yucatan, Mexico. Bull Environ Contam Toxicol 94:58–65

Aspmo K, Berg T, Ferrari C, Gauchard PA, Fain X, Wibetoe G (2006) Mercury in the Atmosphere, Snow and Melt Water Ponds in the North Atlantic Ocean during Arctic Summer. Environ Sci Technol 40:4083–4089

Brosset C (1987) The behavior of mercury in the physical environment. Water Air Soil Pollut 34(2):145–166

Brunke EG, Labuschagne C, Ebinghaus R, Kock HH, Slemr F (2010) Gaseous elemental mercury depletion events observed at Cape Point during 2007–2008. Atmos Chem Phys 10(3):1121–1131

Carpi A, Lindberg SE (1998) Application of a teflon dynamic flux chamber for quantifying soil mercury flux: tests and results over background soil. Atmos Environ 32:873–882

De La Rosa DA, Volke-Sepulveda T, Solorzano G, Green C, Tordon R, Beauchamp S (2004) Survey of atmospheric total gaseous mercury in Mexico. Atmos Environ 38:4839–4846

Draxler, R R (1999) HYSPLIT4 User's Guide, NOAA Tech. Memo, ERLARL-230, NOAA Air Resources Laboratory, Silver Spring. Last revised April 2013

Fritz B, Matthew Barnett J, Snyder S, Bisping L, Rishel J (2015) Development of criteria used to establish a background environmental monitoring station. J Environ Radioact 143:52–57

Fu X, Feng X, Zhu W, Wang S, Lu J (2008) Total gaseous mercury concentrations in ambient air in the eastern slope of Mt. Gongga, South-Eastern fringe of the Tibetan plateau, China. Atmos Environ 42(5):970–979

Fu XW, Feng X, Liang P, Zhang H, Ji J, Liu P (2012) Temporal trend and sources of speciated atmospheric mercury at Waliguan GAW station, Northwestern China. Atmos Chem Phys 12(4):1951–1964

García R, C del Torres Ma, Padilla H, Belmont R, Azpra E, Arcega-Cabrera F, Báez A (2006) Measurements of the trace metals and inorganic ions in Rancho Viejo a rural wooded area in the state of Mexico, Mexico. Atmos Environ. 40(32):6088–6100

Global Mercury Observation System (GMOS) (2013) Institute of Atmospheric Pollution Research, Italy and European Commission., http://www.gmos.eu/

Iverfeldt Å (1991) Occurrence and turnover of atmospheric mercury over Nordic countries. Water Air Soil Pollut 56(2013):251–265

Kellerhals M, Beauchamp S, Belzer W, Blanchard P, Froude F, Harvey B, Tordon R (2003) Temporal and spatial variability of total gaseous mercury in Canada: results from the Canadian Atmospheric Mercury Measurement Network (CAMNet). Atmos Environ 37(7):1003–1011

Kennett RJ, Korb KB, Nicholson AE (2001) Seabreeze prediction using Bayesian networks. In: Advances in Knowledge Discovery and Data Mining. Springer, Berlin, pp 148–153

Kim M-Y, Kang H-G, Park S-B (1987) Study of the distribution and behavior of mercury in ambient air. J Korean Air Pollut Res Assoc 13(2):9–24

Kock HH, Bieber E, Ebinghaus R, Spain TG, Thees B (2005) Comparison of long-term trends and seasonal variations of atmospheric mercury concentrations at the two European coastal monitoring stations Mace Head, Ireland, and Zingst, Germany. Atmos Environ 39(39):7549–7556

Lee DS, Dollard GJ, Pepler S (1998) Gas-phase mercury in the atmosphere of the United Kingdom. Atmos Environ 32:855–864

Lindberg S, Bullock R, Ebinghaus R, Engstrom D, Feng XB, Fitzgerald W, Pirrone N, Prestbo E, Seigneur C (2007) A synthesis of progress and uncertainties in attributing the sources of mercury in deposition. Ambio 36(1):19–32

Lindqvist O, Rodhe H (1985) Atmospheric mercury—a review. Tellus B 37(3):136–159

Lu JY, Schroeder WH (2004) Annual time-series of total filterable atmospheric mercury concentrations in the Arctic. Tellus 56B:213–222

Marquez-Estrada (2011) Characterization of the Celestún site: meteorology and potential mercury sources. Technical Report of Celestún

Mason RP, Reinfelder JR, Morel FMM (1995) Bioaccumulation of mercury and methylmercury. Water Air Soil Pollut 80(1-4):915–921

Petersen G, Iverfeldt Å, Munthe J (1995) Atmospheric mercury species over central and northern Europe; model calculations and comparison with observations from the Nordic air precipitation network for 1987 and 1988. Atmos Environ 29:47–67

Pirrone N, Mason RP (eds) (2009) Mercury fate and transport in the global atmosphere: emissions, measurements and models. Springer, Berlin

Poissant L (2000) Total gaseous mercury in Québec (Canada) in 1998. Sci Total Environ 259:191–201

Schmolke SR, Schroeder WH, Kock HH, Schneeberger D, Munthe J, Ebinghaus R (1999) Simultaneous measurements of total gaseous mercury at four sites on a 800 km transect: spatial distribution and short-time variability of total gaseous mercury over central Europe. Atmos Environ 33:1725–1733

Schroeder WH, Munthe J (1998) Atmospheric mercury an overview. Atmos Environ 32:809–822

SEDUMA-Yucatán (Secretaria de Desarrollo Urbano y Medio Ambiente del Estado de Yucatán) (2009) Programa estatal para la prevención y gestión integral de los residuos 2009-2012. Gobierno del Estado de Yucatán, México, p 125, Available in: http://www.semarnat.gob.mx/sites/default/files/documentos/gestionresiduos/pepgir_yucatan.pdf

Soler-Bientz R, Watson S, Infield D (2010) Wind characteristics on the Yucatán Peninsula based on short term data from meteorological stations. Energy Conversion Manag 51:754–764

Sprovieri F, Pirrone N, Ebinghaus R, Kock H, Dommergue A (2010) A review of worldwide atmospheric mercury measurements. Atmos Chem Phys 10(17):8245–8265

Sprovieri F, Gratz LE, Pirrone N (2013) Development of a Ground-Based Atmospheric Monitoring Network for the Global Mercury Observation System (GMOS). In: E3S Web of Conferences, Vol. 1, 17007. EDP Sciences

Stamenkovic J, Lyman S, Gustin MS (2007) Seasonal and diel variation of atmospheric mercury concentrations in the Reno (Nevada, USA) airshed. Atmos Environ 41(31):6662–6672

Temme C, Einax JW, Ebinghaus R, Schroeder WH (2003) Measurements of atmospheric mercury species at a coastal site in the Antarctic and over the south Atlantic Ocean during polar summer. Environ Sci Technol 37:22–31

UNEP (2013) Global Mercury Assessment 2013: sources, emissions, releases and environmental transport. UNEP Chemicals Branch, Geneva

Wan Q, Feng X, Lu J, Zheng W, Song X, Han S, Xu H (2009) Atmospheric mercury in Changbai Mountain area, northeastern China I. The seasonal distribution pattern of total gaseous mercury and its potential sources. Environ Res 109:201–206

Wang Z-W, Chen Z-S, Duan N, Zhang X-S (2007) Gaseous elemental mercury concentration in atmosphere at urban and remote sites in China. J Environ Sci 19:176–180

Weiss-Penzias P, Jaffe DA, Mcclintick A (2003) Gaseous elemental mercury in the marine boundary layer: evidence for rapid removal in anthropogenic pollution. Environ Sci Tech 37:3755–3763

Zhu J, Wang T, Talbot R, Mao H, Hall CB, Yang X, Huang X (2012) Characteristics of atmospheric total gaseous mercury (TGM) observed in urban Nanjing, China. Atmos Chem Phys 12(24):12103–12118